

Green and scalable synthesis of chiral aromatic alcohols through an efficient biocatalytic system

Meng-Nan Han,¹ Xu-Ming Wang,¹ Chao-Hong Pei,¹ Chao Zhang,¹ Zhidong Xu,² Hong-Lei Zhang^{1*} and Wei Li^{1**} 

¹College of Chemistry and Environmental Science, Key Laboratory of Chemical Biology of Hebei Province, Laboratory of Medicinal Chemistry and Molecular Diagnosis of the Ministry of Education, Hebei University, 180 Wusi East Road, Baoding 071002, China.

²Shijiazhuang Vince Pharma Tech Co Ltd Fangda Science and Technology Park, 266 Tianshan Street, Shijiazhuang City, China.

Summary

Chiral aromatic alcohols have received much attention due to their widespread use in pharmaceutical industries. In the asymmetric synthesis processes, the excellent performance of alcohol dehydrogenase makes it a good choice for biocatalysts. In this study, a novel and robust medium-chain alcohol dehydrogenase RhADH from *Rhodococcus* R6 was discovered and used to catalyse the asymmetric reduction of aromatic ketones to chiral aromatic alcohols. The reduction of 2-hydroxyacetophenone (2-HAP) to (*R*)-(-)-1-phenyl-1,2-ethanediol ((*R*)-PED) was chosen as a template to evaluate its catalytic activity. A specific activity of 110 U mg⁻¹ and a 99% purity of *e.e.* was achieved in the presence of NADH. An efficient bienzyme-coupled catalytic system (RhADH and formate dehydrogenase, CpFDH) was established using a two-phase strategy (dibutyl phthalate and buffer), which highly raised the tolerated substrate concentration (60 g l⁻¹). Besides, a broad range of aromatic ketones were enantioselectively reduced to the corresponding chiral alcohols

by this enzyme system with highly enantioselectivity. This system is of the potential to be applied at a commercial scale.

Introduction

Chiral aromatic alcohols are widely used for synthetic procedures in the pharmaceutical and fine-chemical industries (Quaglia *et al.*, 2013). Such an optically active (*R*)-1-phenyl-1,2-ethanediol (PED) is a versatile chiral building block for the synthesis of pharmaceuticals, pheromones, liquid crystals, etc (Li *et al.*, 2013). Several procedures are available for obtaining optically pure alcohols like enzymatic resolution, reduction of ketones with chiral reductants and catalytic reduction of ketones with biocatalysts (Matsunami *et al.*, 2018). In all these processes, the optical purity and the yield are the objective the researchers pursue. Enzymatic resolution is rarely found in practical application due to its low utilization of raw material. Chiral reduction is limited because of the enantioselectivity, cost of the chiral reductants and environmental issues although it is widely used in commercial production (Hodgkinson *et al.*, 2014). Biocatalytic reduction seems to be the most potential and competitive industrialization process compared with chemical catalysis due to its clean and ecofriendly way, mild reaction conditions and high selectivity for the substrate, which is reflected in the application of some important products (Şahin and Dertli, 2017). It is reported that the chiral compounds produced by biocatalytic reduction accounted for 20% of the total chiral alcoholic intermediates in industrial products (Honda *et al.*, 2017).

Biocatalysis can be performed by using whole-cell microorganism or isolated enzymes as both methods have some advantages and drawbacks (Öksüz *et al.*, 2018). Whole-cell biocatalysts are easy to obtain and relatively cheap and more stable, but its catalytic reaction is subject to the influence of other metabolic reactions in the cell, which produce other by-products, affecting the separation and purification of the target products (Şahin, 2019). Isolated enzymes are highly selective and recyclable catalyst. Although they are expensive, the catalytic efficiency is extremely high and the product obtained by catalysis is convenient for separation and purification (Şahin, 2018). Thus, enzymatic catalysis shows great application prospects. Extensive research

Received 10 December, 2019; revised 2 May, 2020; accepted 11 May, 2020.

For correspondence. *E-mail zhanghonglei@hbu.edu.cn; Tel./Fax +86 312 5929009. **E-mail liweihebeilab@163.com; Tel./Fax +86 312 5929009.

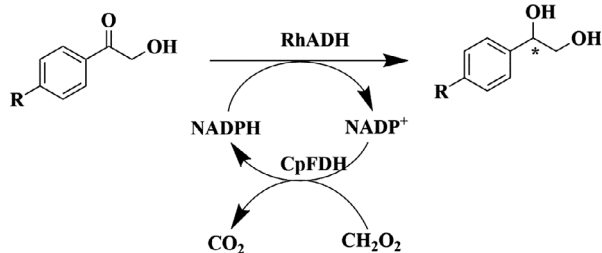
Microbial Biotechnology (2021) 14(2), 444–452
doi:10.1111/1751-7915.13602

Funding information

This work was financially supported by the Natural Science Foundation of Hebei Province (grant number B2016201031), the Hebei Province Science Foundation for High-level Personnel (grant number GCC2014013), the Hebei University Science Foundation (grant number 3333112, and the Post-graduate's Innovation Fund Project of Hebei University (grant number hbu2019ss007).

has been carried out with the use of enzyme as biocatalysts in bioreduction processes, and many exemplary biocatalytic reaction processes were developed and examined (Du *et al.*, 2014). It is found from current reports that various naturally evolved or tailor-made alcohol dehydrogenases have been successfully applied in pharmaceuticals, agrochemicals and liquid materials (Zhang *et al.*, 2014; Chen *et al.*, 2015; Cui *et al.*, 2017). Rocha-Martín *et al.* identified a short-chain alcohol dehydrogenase from *Thermus thermophilus* HB27 (Rocha-Martín *et al.*, 2012). This enzyme coupled to an immobilized cofactor recycling partner was utilized for the quantitatively asymmetric reduction of rac-2-phenylpropanal to (*R*)-2-phenyl-1-propanol with an enantiomeric excess of 71%. Tentori *et al.* (2018) also reported two alcohol dehydrogenases (ADHs) for the reduction of aromatic and aliphatic nitroketone. The enantioselectivities of 62–99% *e.e.* can be achieved with these two specific ADHs, affording either the (*S*) or (*R*)-enantiomer of the corresponding nitroalcohols. Yue obtained an alcohol dehydrogenase from *Kluyveromyces polysporus* (KpADH) with mutation of S237 (Yue *et al.*, 2018). The S237 variant exhibited fine tuning of the substrate specificity and enantioselectivity and could asymmetrically reduce several ketones with > 99% *e.e.* As more alcohol dehydrogenases are discovered and stereospecific reduction systems are established, the researchers are increasingly paying attention to the structure characterization, catalytic activity and efficiency of enzymes in order to raise the concentration of substrates and shorten the conversion time in the consideration of industrial application. Therefore, we attempt to build a catalysis platform of alcohol dehydrogenase and coenzyme to catalyse 2-hydroxyacetophenone (2-HAP) and its derivatives to generate corresponding chiral alcohols (Fig. 1).

In this research, a novel medium-chain alcohol dehydrogenase (RhADH) was isolated and purified after *Rhodococcus* sp. R6 was obtained by fermentation



R: H, F, Cl, Br, OMe

Fig. 1. Biosynthetic pathway for the production of chiral aromatic alcohols from carbonyl compounds via the dual-enzyme coupled system.

under optimal conditions. The reduction of 2-HAP to (*R*)-PED was used as a template to verify the activity of RhADH. An alcohol dehydrogenase and formate dehydrogenase coupled coenzyme regeneration system (RhADH-CpFDH) are found to be an efficient biocatalytic combination. Biphasic catalytic conversion system is more appropriate for increase of substrate concentration and conversion. A high substrate concentration, excellent enantioselectivity and satisfied conversion are achieved with the template bioreduction process. A series of aromatic alcohol is prepared within the system. The current study offers a practical method for preparation of chiral aromatic alcohols in commercial scale.

Results and discussion

Assay for sequence and structure of alcohol dehydrogenase

The strategy of genome hunting has been widely used to find desired enzymes for bioreduction of ketones to corresponding chiral alcohols. The reported genomes of *Rhodococcus erythropolis* strain CCM2595 (GCF_000454045.1) revealed the presence of 58 open reading frames (ORF) that encode putative dehydrogenases/oxidoreductases. Based on the gene sequence of putative dehydrogenases/oxidoreductases, a primer was designed and the genome of *Rhodococcus* R6 was homologously amplified with the primer. After amplification, five possible fragments of alcohol dehydrogenase gene were obtained and expressed in *E. coli*. Through the analysis of conversion for the substrate (2-HAP; Table S1), it was found that one of the recombinant bacteria had the activity to convert substrate. Furthermore, the inserted gene fragments of the recombinant strain were sequenced and a 1047-bp gene fragment was achieved, which was named as *rhadh*. This gene contained open reading frames encoding polypeptides of 348 amino acids with a predicted molecular weight of 36.19 kDa. BLASTn results indicated that RhADH shares significant sequence similarity (30–99%) with NAD(P)-dependent medium-chain alcohol dehydrogenases in the NCBI database, suggesting that RhADH is a member of the medium-chain alcohol dehydrogenase family (MDR). Amino acid sequence analysis of RhADH using the conserved domains tool in NCBI is illustrated in Figure S1, which means that the amino acid sequence consists of an NAD (H)-binding domain at the site of GxGxxG (72-77). Homologous modelling showed that the enzyme has four monomers and contains eight zinc-binding sites. Each subunit is composed of a cofactor-binding domain and a catalytic domain (Fig. S2). Each subunit has two tightly bound zinc atoms, a structural zinc in a lobe of the catalytic domain and a catalytic zinc at the active site.

Purification and enzymatic properties of RhADH

After fermentation of recombinant *E. coli* BL21 (DE3)/pGEX-4T-1-*rhadh*, the crude enzyme of RhADH was harvested using cell lysis and centrifugation. Crude enzyme was further purified using an affinity chromatography system equipped with GSTrap HP. The purified recombinant protein RhADH was monitored by SDS-PAGE (Fig. S3). It has been confirmed that RhADH was a single band with a molecular size of approximately 60 kDa, which is compatible with the presence of the GST tags (26 kDa). The enzymatic assay revealed that RhADH was a coenzyme (NADH)-dependent enzyme. It exhibited a specific activity of 110 U mg⁻¹ when 2-HAP was used as the substrate. After tested with the conversion of 2-HAP to (*R*)-PED under the catalysis of RhADH, it was further confirmed that RhADH follows the deductive catalytic mechanism above. The optical purity of (*R*)-PED was 99% (Fig. S4). The optimal temperature and pH for the activity of purified RhADH were 45°C and 7.5, respectively (Fig. S5), suggesting that RhADH has certain heat resistance and is susceptible to environmental pH.

Metal ions play an important role in promoting the catalytic activity of the enzyme (Zhang *et al.*, 2011). RhADH showed the highest conversion activity (Table S2) especially in the presence of Zn²⁺ in solution. This result also fully confirmed that RhADH is a zinc-dependent alcohol dehydrogenase. Ca²⁺ and Mg²⁺ exhibited moderate activity. On the contrary, Mn²⁺, Na⁺, K⁺ and Cu²⁺ metal ions inhibited the activity of the enzyme. These metal ions might destroy the structure of enzyme activity centre after binding with enzyme, eventually causing the decrease and even the loss of enzyme activity.

Optimization of catalytic conversion system

According to the catalytic properties of RhADH depending on coenzyme NADH, a double-enzyme coupled catalytic system (RhADH and formate dehydrogenase CpFDH) was investigated and optimized (Fig. 2). The activity of the catalytic system depended on the ratio of the two enzymes; as the proportion of RhADH and CpFDH increased, the bioconversion efficiency was raised. When the ratio of RhADH and CpFDH reached 1:10, the bioconversion rate was 98.3% (1.0 g l⁻¹ 2-HAP). The bioconversion efficiency decreased with the increasing of the ratio at more than 1:10 (Fig. 2A), which might be attributed to the increase of coenzyme ratio that affect the contact between RhADH and substrate, resulting in the decrease of bioconversion efficiency. Therefore, the ratio of RhADH to CpFDH at 1:10 was selected to be used for further solvent system study.

The composition of solvents played a key role in the activity of the catalytic system. The solubility of substrate in aqueous solution was very small, and most of the substrate was suspended in water, which made the enzyme unable to conduct effective catalytic conversion. By using water/organic solvent two-phase system, the reaction concentration of the substrate was raised and the catalytic reaction proceeded between the two phases (Zhang *et al.*, 2019). In order to select and evaluate suitable organic solvents, log *P* value was used as the evaluation index of solvent polarity, i.e. logarithmic value of partition coefficient of a solvent in standard water/*n*-octanol system. Table 1 describes the conversion of RhADH-CpFDH in a two-phase system containing organic solvents with log *P* values of 1–6. The results showed that when the organic solvent with log *P* < 2 was used, the conversion rate of the two enzymes was low, for example, in the two-phase system containing ethyl acetate and *n*-hexanol. The solvent with log *P* < 2 has high polarity and good solubility with water, which easily caused deactivation of biocatalysts. Therefore, these organic solvents were not suitable for biocatalytic reaction systems. When log *P* of organic solvents was greater than 4, the conversion of substrates became higher. Low polar solvents had little effect on biocatalysts. When dibutyl phthalate was used as organic phase, the conversion rate (75.3%, 5.0 g l⁻¹ 2-HAP) was higher than that of other organic solvents. Dibutyl phthalate was chosen as the best organic solvent in the two-phase system.

In addition, the partition ratio of organic phase to water phase was studied to determine the optimum catalytic conditions. As shown in Figure 2B, RhADH-CpFDH reached the highest bioconversion efficiency of 85.1% using an aqueous phase to organic phase ratio of 3:1. As the ratio increased, bioconversion decreased slightly. Thus, aqueous: organic phase ratio of 3:1 was chosen as the optimal ratio for bioconversion in a two-phase system.

Finally, the initial concentration of 2-HAP in this two-phase system was tested. When the substrate concentration was 5.0 g l⁻¹, the bioconversion of the two-enzyme system was 84.6%. As the substrate concentration increased, the bioconversion increased. When the substrate concentration reached 60.0 g l⁻¹, the bioconversion reached a maximum of 99.0%. As the substrate concentration increased further, the conversion rate decreased. The bioconversion rate was only 60.8% for a substrate concentration of 70.0 g l⁻¹ (Fig. 2C). The *e.e.* values for all of the products reached above 99%. Under the condition of constant enzyme concentration, when the substrate concentration was low, the enzyme was not saturated by the substrate, and the conversion rate was relatively low. With the increase of substrate

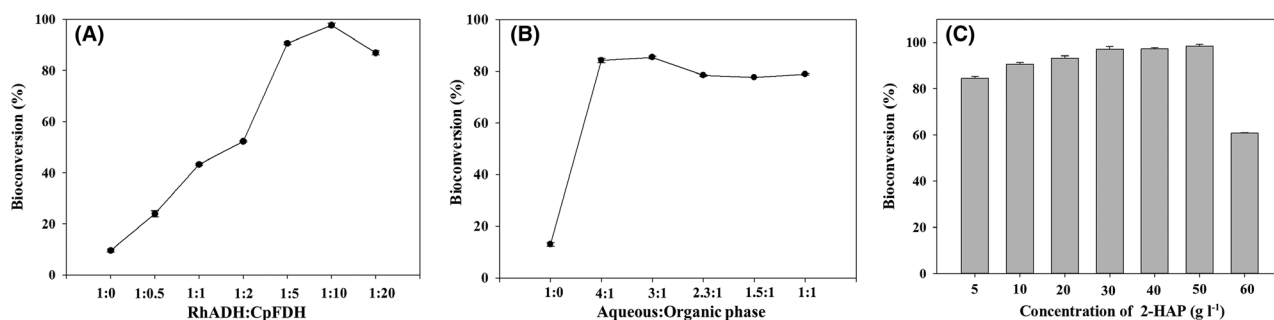


Fig. 2. Optimization of the enantioselective reduction system by the RhADH-CpFDH coupling enzyme in a two-phase system.

A. Effect of various ratios of RhADH to CpFDH in the enantioselective reduction system.

B. Effect of various ratios of water phase: organic phase in the two-phase system.

C. Influence of the initial concentration of 2-HAP in the catalytic system.

Table 1. Effects of organic solvents on bioconversion by the RhADH-CpFDH coupling system in a two-phase catalytic system.

Organic solvents	Log <i>P</i> value	Bioconversion (%)
Non	–	47.6 ± 1.0
Dibutyl phthalate	5.4	75.3 ± 1.3
Decanoic acid ethyl ester	4.9	44.9 ± 1.4
Ethyl laurate	5.7	45.0 ± 1.2
<i>n</i> -heptane	4.0	48.9 ± 1.2
Ethyl acetate	0.7	7.4 ± 0.2
<i>n</i> -hexanol	1.8	29.6 ± 0.9
<i>n</i> -hexane	3.9	46.3 ± 1.1

concentration, the enzymes in the solution were gradually bound by the substrate, and the conversion rate also increased. When the substrate concentration was relatively high, the enzymes in the solution were completely saturated by the substrate. No conversion increase was observed even if the substrate concentration was raised further. On the contrary, excessive substrate concentration affected the activity of the enzyme and made the conversion rate decrease. Therefore, the optimal initial concentration of 2-HAP was set at 60.0 g l⁻¹ for (*R*)-PED production. On the basis of optimal catalytic conditions, the bioconversion and preparation of (*R*)-PED were examined. The bioconversion was scaled up, and 6.0 g of 2-HAP was converted in the system (100 ml). After conversion and work-up, the desired product was obtained with the yield of 98% and *e.e.* of 99%, which was higher than that catalysed by (*R*)-specific carbonyl reductase RCR (95.4% *e.e.*; Zhang *et al.*, 2011) and reductase HEPR from *Saccharomyces cerevisiae* JUC15 (92.4% *e.e.*; Hu *et al.*, 2010).

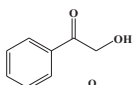
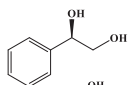
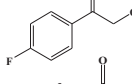
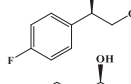
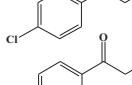
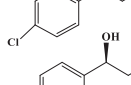
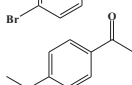
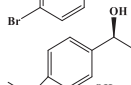
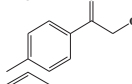
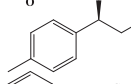
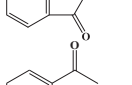
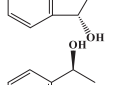
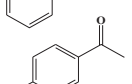
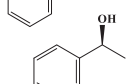
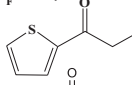
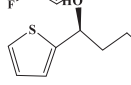
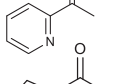

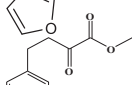
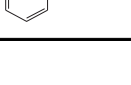
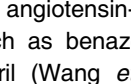

Application of bienzyme-coupled two-phase catalytic system

We also studied the conversion of other carbonyl compounds with two-phase catalytic system coupled by two enzymes. First, the effect of substituents on the catalytic

activity of the enzyme was investigated. There has been reported that when the substituents on the phenyl ring of *alpha*-hydroxyacetone are in the *ortho*- or *meta*-position, the steric hindrance of the substituents has a great influence on the activity of the enzyme and also on the electron cloud density of the phenyl ring. The same conclusion can be drawn from our simulation calculation. Therefore, we only studied *para*-substituted substrates. As shown in Table 2, the double-enzyme catalytic system exhibited good catalytic activity (100%) when the *para*-position of benzene ring was replaced by electron-withdrawing group (F, -Br, or -Cl). When the benzene ring is substituted with the electron-donating group (CH₃ and OCH₃), the double-enzyme catalytic system exhibits poor conversion activity (< 40%). From the above results, it can be seen that the electron cloud density of carbonyl group has a great influence on the activity of enzymes. The lower the electron cloud density of carbonyl group is, the more conducive to carbonyl reduction. The higher the electron cloud density of carbonyl group is, the less conducive to carbonyl reduction. Second, we studied the effect of the *alpha* position of carbonyl group on the catalytic activity of the double-enzyme system. When the hydroxyl group is replaced by Cl, the catalytic activity of the double-enzyme system decreases slightly. When the hydroxyl group is replaced by hydrogen, the activity of enzyme is not affected. The reduction of heterocyclic aromatic ketones was explored with this system. The enzymatic system showed poor activity for the reduction of thienyl ketones (36.5%). However, the enzyme system completely lost its activity when used in 10a and 11a. It can be inferred that the heterocyclic structure increases the electron cloud density of carbonyl group and cannot effectively bind to the active centre of the enzyme, thus losing its activity.

We applied this enzyme catalytic system to the reduction of non-aromatic ketones. 12a was reduced to 12b with the two-phase catalytic system. 12b is an important

Table 2. Application of bienzyme-coupled two-phase catalytic system.

Influence of substituted group	Non	Substrate (a)	Product (b)	AverageBioconversion (%)	<i>e.e.</i> (%)
EWG at 4'-position	1			99.3	> 99 (<i>R</i>)
	2			100	> 99 (<i>R</i>)
	3			100	> 99 (<i>R</i>)
EDG at 4'-position	4			100	> 99 (<i>R</i>)
	5			23.5	> 99 (<i>R</i>)
Substituted group at α -position	6			38.38	> 99 (<i>R</i>)
	7			69.2	> 99 (<i>R</i>)
Aromatic Heterocycles	8			100	> 99 (<i>S</i>)
	9			100	> 99 (<i>S</i>)
	10		—	0	—
	11		—	0	—
Non-aryl ketone	12			100	> 99 (<i>R</i>)

intermediate for the synthesis of many angiotensin-converting enzyme inhibitors (ACEIs), such as benazepril, delapril, enalapril, lisinopril and ramipril (Wang *et al.*, 2018). After catalytic conversion and purification, preparative sample of 12b was obtained with a yield of 81.2% and an *e.e.* of 99%. The product was then identified and characterized (Fig. S6). The optical rotation of 12b achieved was measured as -13.2 ($c = \text{neat}$) at 25°C . The reported value of 12b was $[\alpha]_{\text{D}}^{25} = -9.3^\circ$ ($c = \text{neat}$; Arrigo *et al.*, 2010). Much more work is being conducted to scale up the catalytic reaction in a commercial purpose for the chiral compound.

Analysis of molecular docking

Generally, ADHs possess a limited substrate range defined by the three-dimensional structure of the active site in each enzyme (Anna, 2010). However, RhADH

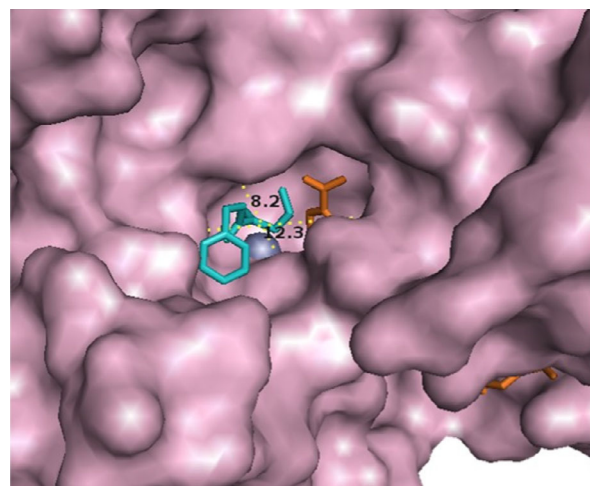


Fig. 3. Estimation of substrate entry of RhADH using homology-based models. The different colours represent corresponding substances, green: 2-HAP; yellow: active sites; grey: zinc atom; orange: NADH; blue: ethyl 2-oxo-4-phenylbutyrate.

has a broad spectrum of substrates in this coupled system, which could be explained by the size of the substrate entry of RhADH. 12a as a substrate was docked into the enzyme (RhADH) active sites properly. The results revealed that the average diameter of the RhADH substrate entrance site was 10.25 Å (Fig. 3). Thus, RhADH exhibited a broader substrate scope in the reduction of complex substrates, suggesting the higher commercial application value of RhADH. From the perspective of the environment and economy, this biosynthesis method is of great application prospects, making it an ideal green and sustainable synthesis route.

Conclusions

A unique medium-chain alcohol dehydrogenase RhADH was obtained, which exhibited excellent activity and enantioselectivity for reduction of 2-HAP. The biocatalytic process was improved using the RhADH-CpFDH coupled system in a two-phase approach. The yields of (*R*)-PED (60 g l⁻¹) were significantly higher than any other biocatalysts reported so far. Moreover, the enzyme system exhibited high enantioselectivity in catalysing various aromatic ketones in high substrate concentration, thereby highlighting its potential applications for the industrial synthesis of chiral alcohols. It suggests that this newly constructed catalytic system offers a novel possibility for the commercial production of a wide range of chiral alcohols.

Experimental procedures

Microorganisms and chemicals

Rhodococcus sp. R6 was preserved in our laboratory. *E. coli* strains, DH5 α and BL21(DE3), were used as the host cells. Cofactors and all the carbonyl compounds and their corresponding chiral alcohols were purchased from Sigma-Aldrich (Milwaukee, WI, USA) and Aladdin (Shanghai, China), respectively. Restriction enzymes were purchased from Takara Shuzo (Kyoto, Japan). All other reagents used were of analytical grade.

Cloning and expression of alcohol dehydrogenase

Primers were designed using Primer Premier version 5.5 (Premier, Palo Alto, CA, USA) based on the putative sequence of oxidoreductase from the registered *Rhodococcus erythropolis* strain CCM2595 (GCF_000454045.1) in the NCBI database (Table S3). The DNA fragment of the reductase gene was amplified and then inserted into the expression vector pGEX-4T-1. The resulting plasmid was transformed into *E. coli* BL21 (DE3). The activity towards 2-HAP using whole cells of recombinant *E. coli* was tested to choose an effective

reductase. Subsequently, the purified amplification product and the plasmid were verified by DNA sequencing. Finally, a recombinant *E. coli* BL21 (DE3)/pGEX-4T-1-*rhadh* and the *rhadh* gene, encoding alcohol dehydrogenase RhADH, were obtained. Recombinant protein RhADH was purified using a purifier system (ÄKTA pure; GE Healthcare) equipped with GStrap HP (GE Healthcare, Piscataway, NJ, USA). The detailed operation was referenced to the protocol (Zhang *et al.*, 2019).

Assay of enzyme activity

BCA protein assay kit (Sangon Biotech (Shanghai)) was used to determine the recombinant protein concentration. The activity of RhADH was assayed by measuring the change of NADH (NADPH) absorbance at 340 nm for 1 min on a Multi-Detection Microplate Reader (Synergy HT; BioTek, Winooski, VT, USA). The reaction mixture (0.1 ml) included 0.1 M KHPO₄ buffer (pH 7.5), 2 μ M NADH (NADPH), 2 μ M 2-HAP, and the appropriate enzyme. One unit (U) of enzyme activity was defined as the amount of enzyme that catalysed the formation and oxidation of 1 μ mol of NADH (NADPH)/min. Effects of pH, temperature and various metal ions on enzymatic activity were investigated as in a previous study (Zhang *et al.*, 2019). Each experiment was performed in triplicate.

Homology modelling and molecular docking

Homology-built models for RhADH were generated separately based on the crystal structures of *R. ruber* ADH-A (PDB ID: 6ffx.1), using the SWISS-MODEL workspace (<https://swissmodel.expasy.org/>), and visualized using PyMOL. Docking procedures were performed according to the methodology described in AutoDock v4.2.6 (Seeliger and de Groot, 2010). The protein structure of RhADH was used to build the receptors, and the substrate 2-HAP and ethyl 2-oxo-4-phenylbutyrate were used as the ligand, respectively. The docking grid box was chosen based on previous studies (Karabec *et al.*, 2010).

Construction of the RhADH and CpFDH dual-enzyme coupled system

The recombinant protein CpFDH from *Candida parapsilosis* C5 was purified by a purifier system (ÄKTA pure; GE Healthcare) with an affinity column filled with pre-charged Ni Sepharose™ (HisTrap HP; GE Healthcare, Piscataway, NJ, USA; Fig. S6) in our previous study (Zhang *et al.*, 2018). The activity of CpFDH was assayed by measuring the increase in absorbance at 340 nm. The reaction mixture (0.1 ml) for the enzyme assay included 0.1 M sodium formate, 1 mM NAD⁺, 0.1 M

KHPO₄ buffer (pH 7.5), and the appropriate enzyme. The specific activity of this enzyme was 70 U mg⁻¹.

Purified RhADH and CpFDH (100 µl each) were added to a potassium phosphate buffer reaction system (1 ml) containing 1.0 g l⁻¹ 2-HAP, 1.0 g l⁻¹ sodium formate and 2 mM NAD⁺. The reaction system was converted at 37°C and 200 r min⁻¹ for 2 h. After the reaction was completed, the supernatant was centrifuged, and 100 µl of supernatant was added to dissolve in 900 µl of methanol solution. Finally, the mixture was analysed by an HPLC system (Ultimate 3000; Thermo Fisher, Waltham, MA) equipped with a Daicel Chiralpak OD–RH column (4.6 × 250 mm, 5.0 µmol l⁻¹; Daicel, Osaka, Japan) and a UV detector. The flow rate was 1.0 ml min⁻¹ with a linear gradient of 0.05% trifluoroacetic acid (phase A) and acetonitrile (phase B) by the following method: 0–10 min (20% B), 10–11 min (20–90% B), 12–16 min (90% B), 17–18 min (90–35% B) and 19–22 min (35%B). All experiments were performed in triplicate. Statistical analysis was performed by one-way analysis of variance with the least significant difference post hoc test, using SPSS ver. 19.0 (IBM, Armonk, NY).

Optimization of catalytic conditions for the dual-enzyme coupled system

First, the ratio of alcohol dehydrogenase to formate dehydrogenase was evaluated. In the bioconversion reaction mixture described above, purified RhADH and CpFDH were added at enzyme activity ratios of 1:0, 1:0.5, 1:1; 1:2, 1:5, 1:10 and 1:20. The optimal ratios of alcohol dehydrogenase to formate dehydrogenase were determined based on the bioconversion of the asymmetric reduction of 2-HAP.

Second, the two-phase catalytic system was optimized. The reaction mixture (10 ml) consisted of 0.1 M potassium phosphate buffer (pH 7.0), which contained 0.5 g l⁻¹ sodium formate, 2 mM NAD⁺, two enzymes (RhADH: CpFDH = 1:10) and an organic solvent (dibutyl phthalate, decanoic acid ethyl acetate, ethyl laureate, *n*-heptane, ethyl acetate, *n*-hexanol and *n*-hexane). The concentration of 2-HAP was 5 g l⁻¹. The ratio of the water phase to organic phase (bioconversion mixture) was 1 to 1. The mixture was stirred at 37°C for 2 h. The organic layer was sampled (100 µl each) and dissolved in 900 µl of methanol. The product content was determined by HPLC. The bioconversion of 2-HAP was also analysed using different ratios of water phase: organic phase (1:0, 4:1, 3:1, 2.3:1, 1.5:1 and 1:1).

Finally, the optimal initial concentration of 2-HAP (5.0, 10.0, 20, 40.0, 60.0 and 70.0 g l⁻¹) in the catalytic system was tested. The concentrations of 2-HAP and (*R*)-PED were analysed by HPLC after 4 h of reaction. The operation was repeated three times.

Asymmetric reduction of carbonyl compounds using the bienzyme-coupled two-phase catalytic system

Reduction experiments using carbonyl compounds with a structure similar to that of the reference substrate 2-HAP were performed. Asymmetric bioreduction of carbonyl compounds was performed using a reaction mixture (10 ml) containing potassium phosphate buffer (0.1 mol l⁻¹, pH 7.0, 7.5 ml), dibutyl phthalate (2.5 ml), carbonyl compound substrates (0.6 g), dual enzyme (17.4 mg RhADH, CpFDH 0.3 g) and 0.1 g of sodium formate. The reaction was performed at 37°C with shaking at 200 r.p.m. The bioconversion and the optical purity of chiral alcohols were determined using HPLC method, in which the corresponding chiral alcohol was as references. In addition, a certain weight of corresponding chiral alcohol standard was added to each sample to be tested as the internal standard, and then, the samples containing the internal standard were analysed by HPLC to verify the configuration of the product.

*Procedure for preparation of (*R*)-PED*

A typical bioconversion system for preparing (*R*)-PED in the optimized dual-enzyme coupled two-phase system was performed as follows. 6 g of 2-HAP (44 mmol) was dissolved in 25 ml of dibutyl phthalate. The solution was added to 75 ml of 0.1 M of potassium phosphate buffer at pH 7.0, which consisted of dual enzyme (174 mg RhADH, CpFDH 3 g) and 1 g of sodium formate. The emulsion was stirred at 37°C for 2 h. After the reaction was complete, the organic phase was taken as the sample for analysis by HPLC to determine the conversion of substrate, the yield of alcohol and the optical purity by comparing the reduced product with the corresponding reference chiral alcohol.

*Procedure for preparation of ethyl (*R*)-2-hydroxy-4-phenylbutyrate*

About 12 g of ethyl 2-oxo-4-phenylbutyrate (58 mmol) was dissolved in 50 ml of dibutyl phthalate. The solution was added to 150 ml of 0.1 M of potassium phosphate buffer at pH 7.0 consisted of dual enzyme (348 mg RhADH, CpFDH 6 g) and 2 g of sodium formate. The emulsion was stirred at 37°C for 2 h. After the catalytic reaction was complete, the oil phase was separated and the aqueous phase was extracted with ethylacetate (200 ml × 2). The combined organic phase was dried over anhydrous sodium sulfate and filtered to remove the salt. The liquid was distilled in a vacuum to remove ethyl acetate and collect ethyl (*R*)-2-hydroxy-4-phenylbutyrate as the product, a colourless liquid. ¹H NMR (400 MHz, CDCl₃) δ (ppm): 7.15–7.31 (m, 5H), 4.16–

4.24 (m, 3H), 2.70–2.82 (m, 2H), 2.08–2.16 (m, 1H), 1.90–2.00 (m, 1H), 1.28 (t, 3H), ^{13}C NMR: 175.24, 141.19, 128.57, 128.43, 126.04, 69.70, 61.78, 35.99, 31.03, 14.20, $[\alpha]_{\text{D}}^{25} = -13.2^\circ$ ($c = \text{neat}$; Fig. S7).

Nucleotide sequence accession number

The nucleotide sequences of *rhadh* and *cpfdh* have been deposited in the GenBank database with accession numbers MG181957 and MG181956.

Acknowledgments

This work was financially supported by the Natural Science Foundation of Hebei Province (grant number B2016201031), the Hebei Province Science Foundation for High-level Personnel (grant number GCC2014013), the Hebei University Science Foundation (grant number 3333112), and the Post-graduate's Innovation Fund Project of Hebei University (grant number hbu2019ss007).

Conflicts of interest

The authors declare no conflict of interest.

References

- Anna, D. (2010) Alcohol dehydrogenase and its simple inorganic models. *Coordin Chem Rev* **254**: 7–8.
- Arrigo, P.D., Pedrocchi-Fantoni, G., and Servi, S. (2010) Chemo-enzymatic synthesis of ethyl (R)-2-hydroxy-4-phenylbutyrate. *Tetrahedron Asym* **21**: 914–918.
- Chen, R., Liu, X., Wang, J., Lin, J., and Wei, D. (2015) Cloning expression and characterization of an anti-Prelog stereospecific carbonyl reductase from *Gluconobacter oxydans* DSM2343. *Enzyme Microb Technol* **70**: 18–27.
- Cui, Z.M., Zhang, J.D., Fan, X.J., Zheng, G.W., Chang, H.H., and Wei, W.L. (2017) Highly efficient bioreduction of 2-hydroxyacetophenone to (S)- and (R)-1-phenyl-1,2-ethanediol by two substrate tolerance carbonyl reductases with cofactor regeneration. *J Biotechnol* **243**: 1–9.
- Du, P.X., Wei, P., Lou, W.Y., and Zong, M.H. (2014) Biocatalytic anti-Prelog reduction of prochiral ketones with whole cells of *Acetobacter pasteurianus* GIM1.158. *Microb Cell Fact* **10**: 84.
- Hodgkinson, R., Jurčik, V., Zanottigerosa, A., Nedden, H.G., Blackaby, A., Clarkson, G.J., and Wills, M. (2014) Synthesis and catalytic applications of an extended range of tethered ruthenium(II)/ η^6 -arene/diamine complexes. *Organometallics* **33**: 5517–5524.
- Honda, K., Inoue, M., Ono, T., Okano, K., Dekishima, Y., and Kawabata, H. (2017) Improvement of operational stability of *Ogataea minuta* carbonyl reductase for chiral alcohol production. *J Biosci Bioeng* **123**: 673–678.
- Hu, Q.S., Xu, Y., and Nie, Y. (2010) Highly enantioselective reduction of 2-hydroxy-1-phenylethanone to enantiopure (R)-phenyl-1,2-ethanediol using *Saccharomyces*

- cerevisiae* of remarkable reaction stability. *Bioresour Technol* **101**: 8502–8508.
- Karabec, M., Łyskowski, A., Tauber, K.C., Steinkellner, G., Kroutil, W., Grogan, G., and Gruber, K. (2010) Structural insights into substrate specificity and solvent tolerance in alcohol dehydrogenase ADH-'A' from *Rhodococcus ruber* DSM 44541. *Chem Commun (Camb)* **46**: 6314–6316.
- Li, Z., Liu, W.D., Chen, X., Jia, S.R., Wu, Q.Q., Zhu, D.M., and Ma, Y.H. (2013) Highly enantioselective double reduction of phenylglyoxal to (R)-1-phenyl-1,2-ethanediol by one NADPH-dependent yeast carbonyl reductase with a broad substrate profile. *Tetrahedron* **69**: 3561–3564.
- Matsunami, A., Ikeda, M., Nakamura, H., Yoshida, M., Kuwata, S., and Kayaki, Y. (2018) Accessible Bifunctional oxy-tethered ruthenium (II) catalysts for asymmetric transfer hydrogenation. *Org Lett* **20**: 5213–5218.
- Öksüz, S., Şahin, E., and Dertli, E. (2018) Synthesis of enantiomerically enriched drug precursors by *Lactobacillus paracasei* BD87E6 as a biocatalyst. *Chem Biodivers* **15**: e1800028.
- Quaglia, D., Pori, M., Galletti, P., Emer, E., Paradisi, F., and Giacomini, D. (2013) His-tagged horse liver alcohol dehydrogenase: immobilization and application in the bio-based enantioselective synthesis of (S)-arylpropanols. *Process Biochem* **48**: 810–818.
- Rocha-Martín, J., Vega, D., Bolivar, J.M., Hidalgo, A., Berenguer, J., Guisán, J.M., and López-Gallego, F. (2012) Characterization and further stabilization of a new anti-prelog specific alcohol dehydrogenase from *Thermus thermophilus* HB27 for asymmetric reduction of carbonyl compounds. *Bioresour Technol* **103**: 43–350.
- Şahin, E. (2018) Production of (R)-1-(1,3-benzodioxol-5-yl) ethanol in high enantiomeric purity by *Lactobacillus paracasei* BD101. *Chirality* **30**: 189–194.
- Şahin, E. (2019) Green synthesis of enantiopure (S)-1-(benzofuran-2-yl)ethanol by whole-cell biocatalyst. *Chirality* **31**: 892–897.
- Şahin, E., and Dertli, E. (2017) Highly enantioselective production of chiral secondary alcohols with *Candida zeylanoides* as a new whole cell biocatalyst. *Chem Biodivers* **14**: e1700121.
- Seeliger, D., and de Groot, B.L. (2010) Ligand docking and binding site analysis with PyMOL and Autodock/Vina. *J Comput Aided Mol Des* **24**: 417–422.
- Tentori, F., Brenna, E., Colombo, D., Crotti, M., Gatti, F.G., Ghezzi, M.C., and Fantoni, G.P. (2018) Biocatalytic approach to chiral β -Nitroalcohols by enantioselective alcohol dehydrogenase-mediated reduction of α -Nitroketones. *Catalysts* **8**: 308.
- Wang, X., Yu, Z., Tang, J., Yi, D., and Chen, S. (2018) Efficient production of (R)-(-)-2-hydroxy-4-phenylbutyric acid by recombinant *Pichia pastoris* expressing engineered d-lactate dehydrogenase from *Lactobacillus plantarum* with a single-site mutation. *Bioprocess Biosyst Eng* **41**: 1383–1390.
- Yue, W., Wei, D., Liu, Y., Zhang, Z.W., Zhou, J.Y., Xu, G.C., and Ni, Y. (2018) Fine tuning the enantioselectivity and substrate specificity of alcohol dehydrogenase from *Kluyveromyces polysporus* by single residue at 237. *Catal Commun* **108**: 1–6.
- Zhang, R.Z., Xu, Y., Xiao, R., Wang, S.S., and Zhang, B.T. (2011) Improvement of (R)-carbonyl reductase-mediated

biosynthesis of (*R*)-1-phenyl-1,2-ethanediol by a novel dual-cosubstrate-coupled system for NADH recycling. *Process Biochem* **46**: 709–713.

Zhang, R., Xu, Y., Xiao, R., Wang, L., and Zhang, B.T. (2014) Optimized expression of (*S*)-carbonyl reductase in *Pichia pastoris* for efficient production of (*S*)-1-phenyl-1,2-ethanediol. *J Basic Microbiol* **54**: 873–879.

Zhang, H.L., Zhang, C., Han, M.N., Pei, C.H., Xu, Z.D., and Li, W. (2018) Efficient biosynthesis of enantiopure tolvaptan by utilizing alcohol dehydrogenase-catalyzed enantioselective reduction. *Green Chem* **20**: 1224–1227.

Zhang, H.L., Zhang, C., Pei, C.H., Han, M.N., and Li, W. (2019) Enantioselective synthesis of enantiopure chiral alcohols using carbonyl reductases screened from *Yarrowia lipolytica*. *J Appl Microbiol* **126**: 127–137.

Supporting information

Additional supporting information may be found online in the Supporting Information section at the end of the article.

Table S1. Bioconversion of 2-HAP by the recombinant strains.

Table S2. Influences of metal ions on the activity of RhADH.

Table S3. Oligonucleotides used in this study.

Fig. S1. Amino acid sequence analysis of RhADH using ESPript tool and conserved domains tool in NCBI.

Fig. S2. Homologous modeling of RhADH. Three-dimensional model was constructed based on the template structure of *R. ruber* ADH-A (PDB ID: 6ffx.1), and the structure

was prepared using the program PyMOL (DeLano Scientific).

Fig. S3. SDS-PAGE analysis of purified RhADH. SDS-PAGE analysis of the recombinant strains, *E. coli* BL21 (DE3)/pGEX-4T-1-*rhadh*, after IPTG induction for 6 h. Gel was stained with 0.05% Coomassie Blue R-250: lane M, molecular weight markers; lane 1, recombinant *E. coli* BL21/pGEX-4T-1-*rhadh* without IPTG introduction; lane 2, recombinant *E. coli* BL21/pGEX-4T-1-*rhadh* with IPTG introduction. lane 3, purified RhADH with a molecular mass of 60 kDa.

Fig. S4. HPLC spectrum of the bioconversion mixture based on the presence of RhADH. a: Standard of 2-HAP, (*R*)-PED, and (*S*)-PED; b: Bioconversion system without the addition of RhADH; c: Bioconversion system with RhADH.

Fig. S5. The influences of temperature and pH on the activity of RhADH. (a) Screening of the optimal temperature for the assay of RhADH activity. (b) Temperature tolerance of RhADH. (c) Screening of the optimal pH for the assay of RhADH activity. (d) pH tolerance of RhADH. The relative activity of RhADH at each optimal temperature and pH for the reduction reactions was defined as 100%.

Fig. S6. SDS-PAGE analysis of purified CpFDH. SDS-PAGE analysis of the recombinant strains, *E. coli* BL21 (DE3)/pet28a-*cpfdh*, after IPTG induction for 6 h. Gel was stained with 0.05% Coomassie Blue R-250: lane M, molecular weight markers; lane 1, recombinant *E. coli* BL21(DE3)/pet28a-*cpfdh* without IPTG introduction; lane 2, recombinant *E. coli* BL21(DE3)/pet28a-*cpfdh* with IPTG introduction. lane 3, purified RhADH with a molecular mass of 40 kDa.

Fig. S7. ¹H NMR, and ¹³C NMR spectra of the ethyl (*R*)-2-hydroxy-4-phenylbutyrate. ¹H NMR (400 MHz, 25°C, CDCl₃), ¹³C NMR (150 MHz, 25°C, CDCl₃).